Science Advances
AAAS

advances.sciencemag.org/cgi/content/full/4/11/eaat5535/DC1

Supplementary Materials for

Entanglement signatures of emergent Dirac fermions: Kagome spin liquid and quantum criticality

Wei Zhu*, Xiao Chen, Yin-Chen He, William Witczak-Krempa

*Corresponding author. Email: phwzhu@gmail.com

Published 9 November 2018, *Sci. Adv.* **4**, eaat5535 (2018)
DOI: 10.1126/sciadv.aat5535

This PDF file includes:

Section S1. EE for free Dirac fermions on the cylinder

The continuum Hamiltonian of Dirac fermions on the infinite cylinder reads

$$H = \sum_{k_y} \int \frac{dk_x}{2\pi} \Psi^\dagger(\vec{k}) \begin{pmatrix} m & k_x - ik_y \\ k_x + ik_y & -m \end{pmatrix} \Psi(\vec{k}) \tag{1}$$

where $\Psi(k) = (\psi_1(k), \psi_2(k))^T$ is a two-component spinor and m is the fermion mass. Here, y is compact with periodicity L_y. The transverse momentum k_y takes discrete values, $k_y = \frac{2\pi n_y + \Phi}{L_y}$, where Φ is the flux inserted in the cylinder.

For an infinite cylinder bipartitioned into 2 semi-infinite cylinders (Fig. S 1), the EE for region A (the left semi-infinite cylinder) obeys an area law with a subleading term, $S = \alpha\,(L_y/\epsilon) - \gamma$. The subleading term, $-\gamma$, will be a function of the flux Φ inserted inside the cylinder [21,27,34].

We briefly review the computation of γ by using the 1d decomposition method discussed in Ref. [27]. The Hamiltonian in Eq. (1) can be written as $H = \sum_{k_y} H^{\rm 1d}(k_y)$, where $H^{\rm 1d}(k_y)$ is a $(1+1)$-dimensional massive Dirac fermion. For a semi-infinite interval, each $H^{1d}(k_y)$ with an effective mass $\sqrt{m^2 + k_y^2}$, contributes an EE [35]

$$S^{\rm 1d}(k_y) = -\frac{1}{12} \ln\left[(m^2 + k_y^2)\epsilon^2\right] \tag{2}$$

ϵ is the short distance UV cutoff. The total EE is then

$$S = -\frac{1}{12} \sum_{k_y} \ln\left[(m^2 + k_y^2)\epsilon^2\right] \tag{3}$$

For the massless case $m = 0$ we are interested in here, by using the Zeta function regularization method, we have

$$S = \alpha \frac{L_y}{\epsilon} - \gamma \tag{4}$$

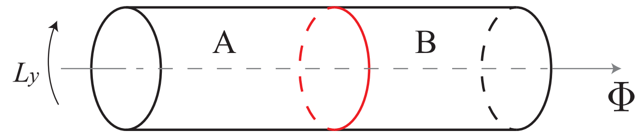

Fig. S 1. Bipartition of an infinite cylinder, which is threaded by a flux Φ.

where the subleading term is equal to

$$\gamma = \frac{1}{6} \ln \left| 2 \sin\left(\frac{\Phi}{2}\right) \right| \tag{5}$$

When $m \neq 0$, the infinite sum in Eq. (3) can also be obtained by using the generalized Zeta function regularization method,

$$\begin{aligned} \sum_{k_y} \ln\left[(m^2 + k_y^2) L_y^2\right] &= \textstyle\sum_{n_y=-\infty}^{\infty} \ln\left[(mL_y)^2 + (2\pi n_y + \Phi)^2\right] \\ &= \ln\left[2\cosh(mL_y) - 2\cos\Phi\right] \end{aligned} \tag{6}$$

This result will be useful when we discuss the EE for the Gross-Neveu model in the next section.

Section S2. EE of interacting Dirac fermions at large N

A. Gross-Neveu quantum critical point

We first briefly review the Gross-Neveu model in the large N limit [36]. The Euclidean Lagrangian for the Gross-Neveu model describing the quantum critical point in our π-flux square lattice Hamiltonian reads

$$\mathcal{L} = -\bar{\Psi}_\alpha \not{\partial} \Psi_\alpha - \frac{g^2}{2(2N)} (\bar{\Psi}_\alpha \tau^z \Psi_\alpha)^2 \tag{7}$$

where the repeated flavor index α is summed over from 1 to N. Ψ_α is a 4-component spinor. For the case of interest to us, $N = 1$, the single 4-component spinor combines the 2 valley and linear band touching degrees of freedom. The large-N extension consists in taking the limit of a large number of valleys. We thus have $(2N)$ 2-component spinors: $\Psi_\alpha^{\mathrm{T}} = (\psi_{\alpha,1}, \psi_{\alpha,2})$, where the $\psi_{\alpha,i}$ have 2 components. $\not{\partial} = \Gamma_\mu \partial_\mu$ with the 2-by-2 Gamma matrices Γ_μ acting on the Lorentz structure but not on the valley indices. The quartic interaction term $(\bar{\Psi}_\alpha \tau^z \Psi_\alpha)^2$ has a relative sign between each pair of valleys due to the Pauli matrix τ^z that acts on the valley degrees of freedom. (To be more precise, we could write the interaction term as $(\bar{\Psi}_\alpha \mathbb{I} \otimes \tau^z \Psi_\alpha)^2$). This is because in the charge density wave phase, half the Dirac fermions acquire a positive mass, while the other half a negative one. If all the masses had the same sign, the system would be a Chern insulator with broken time-reversal symmetry, which is not the case in our lattice model. The above Lagrangian can be decoupled by introducing a Hubbard-Stratonovich field ϕ and yields the Gross-Neveu-Yukawa Lagrangian:

$$\mathcal{L} = -\bar{\Psi}_\alpha(\partial\!\!\!/ + \phi\,\tau^z)\Psi_\alpha + \frac{2N}{2g^2}\phi^2 \tag{8}$$

After integrating out the fermions, the partition function $Z = \int D[\Psi]D[\phi]e^{-S}$ takes the form

$$Z = \int D[\phi] \exp\left[N \,\mathrm{Tr}\ln(\partial\!\!\!/ + \phi\,\tau^z) - \frac{2N}{2g^2}\int d^3x\phi^2\right] \tag{9}$$

In the large N limit, the partition function can be evaluated using the saddle point method,

$$\ln Z = N \,\mathrm{Tr}\ln(\partial\!\!\!/ + \phi\,\tau^z) - \frac{2N}{2g^2}\int d^3x\,\phi^2 \tag{10}$$

Crucially, the saddle point configuration of the ϕ field is determined by solving the gap equation

$$\frac{\langle\phi\rangle}{g^2} = \frac{1}{2}\mathrm{Tr}\left(\frac{\tau^z}{\partial\!\!\!/ + \langle\phi\rangle\,\tau^z}\right) =: \frac{1}{2}\mathrm{Tr}\,G^F(x,x;\langle\phi\rangle) \tag{11}$$

where $G^F(x,x;\langle\phi\rangle)$ is the fermionic Green's function that arises from the saddle point condition. Thus, the fermions acquire a mass given by the saddle point value $\langle\phi\rangle$. At the critical point, this mass vanishes on the infinite plane, but not on the cylinder. The mass will play a crucial role in the computation of the EE, as we shall see below. In momentum space, the gap equation simplifies to

$$\frac{\langle\phi\rangle}{g^2} = 2\int \frac{d^3p}{(2\pi)^3}\frac{\langle\phi\rangle}{p^2 + \langle\phi\rangle^2} \tag{12}$$

At the quantum critical point $\langle\phi\rangle$ vanishes, and the (non-universal) critical coupling is given by

$$\frac{1}{g_c^2} = 2\int \frac{d^3p}{(2\pi)^3}\frac{1}{p^2} \tag{13}$$

where a momentum cutoff should be used.

In order to compute the EE at the quantum critical point, we follow the calculation described in Ref. [28], which makes use of the replica trick [37,38]. Ref. [28] treated the chiral Gross-Neveu model, i.e. without the τ^z in the interaction, while below we adapt the analysis to the non-chiral version. The replica trick allows the calculation of the Rényi entanglement entropies, $S_n = \frac{1}{1-n}\ln \mathrm{Tr}\,\rho_A^n$, for integer values of the Rényi index n. The analytic continuation of S_n to $n=1$, when possible, gives the von Neumann EE: $S = S_{n\to 1}$. The key identity is

$$\mathrm{Tr}\,\rho_A^n = \frac{Z_n}{Z_1^n} \tag{14}$$

where ρ_A is the reduced density matrix of region A, and Z_n is the partition function defined over a special spacetime: an n-sheeted Riemann surface. The n sheets are glued together at the boundary of region A, which in our case is a (flat) circle dividing the cylinder in equal halves. We can formally evaluate the n-sheeted partition function for the Gross-Neveu-Yukawa model:

$$\ln Z_n = N\,\mathrm{Tr}\ln(\partial\!\!\!/_n + \langle\phi\rangle_n\,\tau^z) - \frac{2N}{2g_c^2}\int d^3x\,\langle\phi\rangle_n^2 \tag{15}$$

Around $n \approx 1$, we can expand the saddle point value of ϕ, $\langle\phi(x)\rangle_n$, as

$$\langle\phi(x)\rangle_n \approx m_1 + (n-1)f(x) \tag{16}$$

where m_1 is the self-consistent mass satisfying the gap equation on the physical spacetime, $\frac{1}{2}\,\mathrm{Tr}\,G_1^F(x,x;m_1) = m_1/g_c^2$, and $f(x)$ is an unknown function on the Riemann surface. In the notation used above, $m_1 = m$. Therefore, $\ln Z_n$ can be written as

$$\begin{aligned}\ln Z_n =& N\,\mathrm{Tr}\ln(\partial\!\!\!/_n + m_1\,\tau^z) - \frac{2N}{2g_c^2}\int d^3x_n m_1^2\\ &+ (n-1)N\,\mathrm{Tr}\left(\frac{f(x)\tau^z}{\partial\!\!\!/_1 + m_1\,\tau^z}\right) - (n-1)\frac{2N}{g_c^2}\int d^3x\, m_1 f(x)\end{aligned} \tag{17}$$

In the above expression, if we use Eq. (11), the last two terms will cancel each other. Therefore, we have

$$-\ln\frac{Z_n}{Z_1^n} = -N\left[\mathrm{Tr}\ln(\partial\!\!\!/_n + m_1\,\tau^z) - n\,\mathrm{Tr}\ln(\partial\!\!\!/_1 + m_1\,\tau^z)\right] \tag{18}$$

This is the same result as for a free Dirac fermion with mass m_1. The mass m_1 can be obtained by solving the gap equation at the critical point Eq. (13):

$$\frac{1}{L_y}\sum_{k_y}\int\frac{d^2p}{(2\pi)^2}\frac{1}{p^2+k_y^2+m_1^2} = -\frac{1}{4\pi L_y}\ln\left[2\cosh(m_1L_y) - 2\cos\Phi\right] = 0 \tag{19}$$

Notice that the above result is obtained by using Zeta function regularization which ignores the UV divergent term. To satisfy the above equation, the mass becomes

$$m_1 = \frac{1}{L_y}\mathrm{arccosh}\left(\frac{1}{2} + \cos\Phi\right) \tag{20}$$

If we plug the above expression into Eq. (6) (for the free Dirac fermion EE), we find that $\gamma = 0$ for all values of Φ. Therefore, the subleading term is absent at leading order in N for the Gross-Neveu model in the large N limit. This is the same large-N result as for the chiral Gross-Neveu model [28]. We expect γ to become non-zero at next order in N, $\mathcal{O}(N^0)$.

B. Quantum Electrodynamics (QED3)

The Dirac QSL on the kagome lattice is described by a theory of Quantum Electrodynamics in 3 spacetime dimensions (QED3) in which 4 gapless Dirac fermions are strongly coupled to an emergent gauge field, a_μ. After extending the number of Dirac fermions to N, the Euclidean time Lagrangian becomes:

$$\mathcal{L} = -\bar{\Psi}_\alpha(\partial\!\!\!/ + ia)\Psi_\alpha + \frac{1}{4e^2} f_{\mu\nu} f_{\mu\nu} \tag{21}$$

where $a = a_\mu \Gamma_\mu$ and $f_{\mu\nu} = \partial_\mu a_\nu - \partial_\nu a_\mu$ is the field strength tensor of the gauge field. The repeated flavor index α is summed from 1 to N. Just as for the Gross-Neveu model, this theory is strongly interacting in the long-wavelength limit but becomes tractable at large N. (At large N, the theory is in fact conformally invariant at low energy. Also, we can neglect the monopole operators that result from the compactness of the gauge field in the lattice Hamiltonian.) The leading order large-N solution has the gauge field pinned to its saddle point value. However, in contrast to $\langle\phi\rangle$ in the Gross-Neveu-Yukawa theory on the cylinder, the saddle point value of a_μ vanishes. If present, such an expectation value would generate either a finite fermion density or current, which does not happen on the cylinder (or infinite plane). The n-sheeted partition function is thus simply given by

$$\ln Z_n = N \,\mathrm{Tr} \ln(\partial\!\!\!/_n) + \mathcal{O}(N^0) \tag{22}$$

This is the same answer as for N free gapless Dirac fermions. One subtelty is that the internal gauge field can change the boundary conditions of the fermions in order to lower the system's energy. This means that γ in Eq. (5) is replaced by

$$\gamma = \frac{1}{6} \sum_\alpha \ln \left|2 \sin\left(\frac{\Phi_\alpha^{\mathrm{net}}}{2}\right)\right| \tag{23}$$

where the net flux $\Phi_\alpha^{\mathrm{net}}$ felt by fermion α depends on both the external and internal fluxes. This is discussed in more detail in the main text. At next order in N, the gauge fluctuations will contribute to γ. Such a calculation is beyond the scope of the current paper, but it would be interesting in light of our DMRG results. For example, one would like to know if the $1/N$ correction has the right sign to explain why the observed value exceeds the free Dirac fermion result, $B > 1/6$.

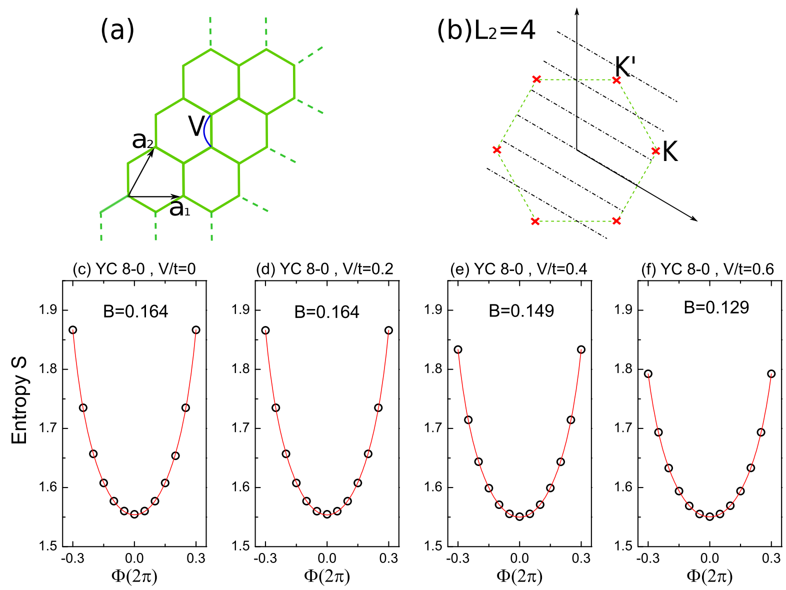

Fig. S2. **Entanglement of quantum critical Dirac fermions on the honeycomb lattice. (a)** Honeycomb lattice on a cylinder with the compact direction being along $\vec{a}_2$. **(b)** Allowed momentum points (dot-dashed lines) in the Brillouin zone for an infinitely long cylinder with circumference $L_2 = 4$ (in unit of lattice vector $\vec{a}_2$). The red crosses mark the positions of the Dirac points. **(c-f)** The entanglement entropy versus the twist parameter Φ on an infinite cylinder with a circumference of 4 unit cells, for various interactions V/t. The red lines are best fits to the scaling function shown in the main text (Eq. 2).

Section S3. Quantum critical point of Dirac fermions on the honeycomb lattice

In the main text, we have studied the fermionic quantum critical point of fermions in the $\pi-$flux square lattice model. In order to confirm that the EE scaling observed is indeed universal, we analyze a different lattice model that is expected to host a quantum critical point in the Gross-Neveu-Yukawa universality class. The model is similar to the π-flux Hamiltonian (Eq. 3 of the main text) but defined instead on the honeycomb lattice. The Hamiltonian contains hopping and repulsion terms:

$$H = t\sum_{\langle ij\rangle}(c_i^\dagger c_j + \text{h.c.}) + V\sum_{\langle ij\rangle} n_i n_j, \tag{24}$$

where $c_i^\dagger$ is the creation operator for a spinless fermion on site i, and n_i is the particle number operator. We focus on the half-filling case. As in the main text, we perform large-scale DMRG simulations on infinite cylinders. The transition from the Dirac semimetal at small V/t to a charge density wave transition occurs at $V_c \simeq 1.36t$ [30,31].

As shown in Fig. S 2(a-b), the allowed momenta of the $L_2 = 4$ (number of unit cells around the circumference) cylinder do not hit the Dirac points ($\vec{K}$ and $\vec{K}'$) at zero flux, thus the entanglement entropy has a minimum at $\Phi = 0$. While the flux deviates from zero, entropy gradually increases,

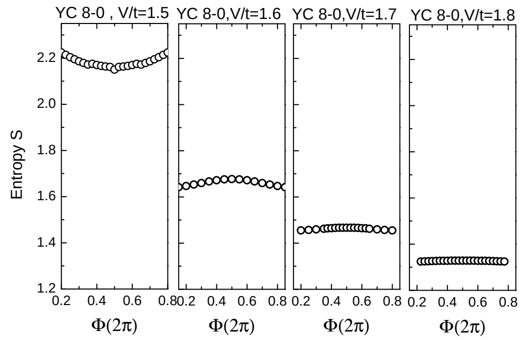

Fig. S3. **Entanglement in the charge-ordered phase**. Entanglement entropy dependence on the external flux in the gapped charge density wave phase, $V > V_c \approx 1.3t$, for the square lattice $\pi-$flux model introduced in the main text.

and becomes maximal approaching $\Phi_c = \pm\frac{2\pi}{3}$, where the momentum lines hit a Dirac point. In Fig. S 2(c-f), we fit the EE using the same scaling ansatz as in the main text. The entanglement entropy dependence on the twisted boundary condition perfectly matches the scaling function, for the whole Dirac semimetal phase. At small V/t, the fitting prefactor B is close to the value for free Dirac fermions, $B = 1/6$, as expected. As the repulsion is increased, B decreases. This behavior was also observed in the square lattice model in the main text, and justified using field theory (see Section and the main text). The agreement between the honeycomb and square lattice DMRG results strongly suggest that our results probe universal low energy properties.

Section S4. EE in the gapped phase

In the main text, we have focused on the non-trivial scaling behavior of the entanglement dependence on the external flux. The strong dependence of the EE on the external flux constitutes a fingerprint of the gapless Dirac cone structure. In this section, we analyze the situation where the Dirac fermions acquire a gap. In the π-flux and honeycomb models, this occurs when the interaction is strong enough $V > V_c$ (V_c is phase transition point).

In Fig. S 3, we show the DMRG data for the EE in the charge density wave phase ($V > V_c$). We observe that the EE has little dependence on the flux Φ, in contrast to the gapless Dirac semimetal occuring at $V < V_c$. This can be understood from the fact that once the system is sufficiently deep in the gapped phase, its correlation length will be smaller than the circumference, and most quantities should be hardly influenced by the twisted boundary conditions. Thus, the EE of the insulating phase is expected to become more insensitive to the flux as the gap increases, which is akin to Thouless's picture of localization in which the energy spectral flow of insulators is robust against boundary conditions. Moreover, in the charge density wave phase $V > V_c$, the EE does not follow the scaling function any more. These results show that the scaling behavior observed at $V < V_c$ is tied to the gapless Dirac fermions.